# 50 Gbit/s PAM4 Data Transmission Over 500-m Single-Mode Fiber Using an 880-nm Single Mode VCSEL

Xing Zhang, *Member, IEEE*, Guorui Zhang, Yue Wen, Wendou Zhang, Hui Li, Yongqiang Ning, Cunzheng Ning, *Fellow, IEEE*, Lijun Wang, and Wenwei Xu, *Senior Member, IEEE*

***Abstract*— Error-free 50 Gbit/s PAM4 data transmission over 500-m single mode fiber was successfully realized using our oxide-confined 880-nm single-mode high-speed VCSELs. This transmission was accomplished because of the flat frequency response of the VCSEL across a wide bias span. Static characteristics and high-speed modulation properties at room temperature and high operation temperature were studied in detail. Data transmission experiments for the 880-nm VCSEL with 4-$\mu$m oxide-aperture diameter was performed. A 50-Gbps PAM4 module was packaged for data transmission. Error-free 50 Gbit/s PAM4 data transmission over 500-m single mode fiber was successfully realized. The proposed VCSEL is fit for the 400G DR8 module because of its 500-m single-channel 50 Gbit/s error-free transmission. Compared with commonly used DML, VCSELs are evidently advantageous in cost and power consumption.**

***Index Terms*— VCSEL, single mode, high speed.**

## I. Introduction

VERTICAL-CAVITY surface-emitting lasers (VCSELs) are commonly used as cost-effective and energy-efficient light sources for short-reach optical interconnects (OIs) in data centers and supercomputers. Given that the operating temperature can reach 80 °C or higher in commercial applications and when costs are considered, VCSEL-based OIs must operate without extra cooling. High performance at high temperature is also important for datacom VCSELs. VCSELs operating at 850 nm are ideal optical sources for short-reach interconnects. These devices are also potential solutions for extended-reach optical links because of their numerous advantages, such as excellent high-speed properties, low power consumption, and low-cost fabrication. As specified in the IEEE 802.3ae 10G Ethernet and IEEE 802.3ba 40G/100G Ethernet standard, directly modulated VCSEL as the standard optical transmitting source for short-reach OIs spans up to 300 m of multimode optical fiber (MMF). Although ∼80%–90% of the optical links used in modern data centers span less than 100 m, expanding the link to longer distances and increasing the per channel bit rate to >50 Gbit/s are clearly needed.

Among various signal modulation formats for VCSEL optical links, pulse amplitude modulation (PAM) has attracted considerable interest because it can take full advantage of the available link bandwidth and achieve data rate transmission beyond the conventional on-off keying limits without considerable increase in the system complexity. PAM4 modulation has high transmission efficiency and low transmission cost due to its four-level modulation format [1]. Szczerba *et al.* demonstrated a 30 Gbit/s PAM-4 link with transmission distance of over 200 m by using a 20 GHz 850-nm multimode VCSEL (MM-VCSEL) [2] and continuously increased the link rate to 94 Gbit/s in the following years [3], [4], [5]. Lavrencik *et al.* achieved 100 Gbit/s error-free transmission with 30 GHz MM-VCSEL using PAM4 modulation and pulse integral type [6]. In 2020, Huang *et al.* used 850-nm MM-VCSEL with a 5.5-$\mu$m oxide aperture to realize 80 Gbit/s transmission of 100-m OM5 multimode fiber through PAM4 modulation [7].

Although MMF transmission links based on MM-VCSEL are widely used, modal dispersion among transverse modes inevitably limits the maximum allowable data rate because of the distortion of transmission configuration [8]. Experimental and theoretical calculations have shown that compared with MM-VCSEL, single-mode VCSELs (SM-VCSEL) reduce the compensation dependence of additional digital signal processing (DSP) on dispersion and relative intensity noise (RIN)-related noise in the optical channel [9]. Qiu *et al.* reported a 1000 m optical link with error-free transmission of up to 28 Gb/s using an 850-nm SM-VCSEL, and the operating temperature was up to 85 °C [10]. Peng *et al.* demonstrated a 500-m optical link that reached a record 40 Gb/s without equalization with an 850-nm SM-VCSEL [11].

Manuscript received 9 August 2022; revised 6 September 2022; accepted 8 September 2022. Date of publication 16 September 2022; date of current version 5 October 2022. This work was supported in part by the National Natural Science Foundation of China under Grant 61874117 and Grant 62090060 and in part by the Jilin Scientific and Technological Development Program under Grant 20200401006GX. *(Guorui Zhang is co-first author.) (Corresponding author: Wenwei Xu.)*

Xing Zhang was with the Changchun Institute of Optics, Fine Mechanics and Physics, Chinese Academy of Sciences, Changchun 130033, China. He is now with Ace Photonics Company Ltd., Changchun 130102, China (e-mail: zhangx@acephoton.com).

Guorui Zhang, Yue Wen, Wendou Zhang, and Wenwei Xu are with Huawei Technologies Company Ltd., Shenzhen 518129, China (e-mail: zhangguorui4@huawei.com; wenyue@huawei.com; zhangwendou@huawei.com; xuwenwei@huawei.com).

Hui Li and Cunzheng Ning are with the College of Integrated Circuits and Optoelectronic Chips, Shenzhen Technology University, Shenzhen 518118, China (e-mail: lihui3@sztu.edu.cn; ningcunzheng@sztu.edu.cn).

Yongqiang Ning and Lijun Wang are with the Changchun Institute of Optics, Fine Mechanics and Physics, Chinese Academy of Sciences, Changchun 130033, China (e-mail: ningyq@ciomp.ac.cn; wanglj@ciomp.ac.cn).

Color versions of one or more figures in this letter are available at https://doi.org/10.1109/LPT.2022.3206902.

Digital Object Identifier 10.1109/LPT.2022.3206902

The effects of chromatic and modal dispersion set the main limitation when the bitrate is increased over long distances. The effects of chromatic dispersion can be reduced by employing VCSELs with a smaller number of transverse modes and consequently narrow spectral width. Various techniques are used to suppress higher-order modes to achieve SM-VCSELs (sidemode suppression ratio [SMSR] >30 dB) or quasi-SM-VCSELs (SMSR≈20 dB) to enable high-speed long-distance data transmission, such as surface relief [12], photonic crystals [13], and Zn diffusion [14]. Among all the available techniques, VCSEL with surface relief (SR) is a simple and effective structure for single-mode operation. This device uses an SR to form an integrated mode filter, allowing for low-spectral width VCSELs with larger oxide apertures. SR-VCSELs offer several advantages, such as a less complex structure than photonic crystal VCSELs, lower differential resistance than small-aperture VCSELs for better impedance matching to 50 Ω loads, and possibly more reliable operation than small-aperture VCSELs (lower current density and internal temperature). In this work, we demonstrate a SM-VCSELs with 4-$\mu$m oxide-aperture diameter and $Si_3N_4$SR. The VCSEL exhibited good mode and temperature characteristics, maintaining a single transverse mode operation at 80 °C with output power of 1.86 mW. Error-free 50 Gbit/s PAM4 data transmission over 500-m single mode fiber was successfully realized using 880 nm VCSEL. The 880nm is one of the working channels specified in the 40G and 100G SWDM4 MSA Technical specifications [15]. The structure of this letter is as follows. First, the structure and fabrication of VCSEL is introduced. Then, the static characteristics of the device are examined. Finally, the dynamic characteristics of the VCSEL analysis and the test results are discussed.

## II. Structure and Fabrication of the 880-nm VCSEL

Fig. 1 shows the device cross-section of the 880-nm VCSEL. The top and bottom distributed Bragg reflector (DBR) consisted of 21 pairs and 37 pairs of $Al_{0.9}Ga_{0.1}As/Al_{0.12}Ga_{0.88}As$ layers, respectively. The active layer had three strained $In_{0.05}Ga_{0.92}As/GaAs$ quantum wells (QWs) with lasing wavelength covering 880 nm. On the active layer, an oxide-confined aperture with 4-$\mu$m diameter was formed to achieve single-transverse-mode lasing. In order to achieve high-speed operation, a double oxide layer configuration is adopted to reduce the parasitic capacitance of VCSEL. The device had a coplanar electrode configuration. All etched trenches were filled with benzocyclobutene (BCB), and $Si_3N_4$ was selected as the insulating layer material.

The distribution of transverse modes in the VCSEL can be calculated using Maxwell's equations [16], [17]. A maximum of five transverse modes can exists for a VCSEL with 4-$\mu$m diameter oxide aperture. Higher-order mode will appear at high injection current. To keep the VCSEL working in single transverse mode under high injection current, a reversed SR structure was adopted to filter the high-order mode. A dielectric film inverting layer with specific thickness was grown on the VCSEL surface to increase the threshold

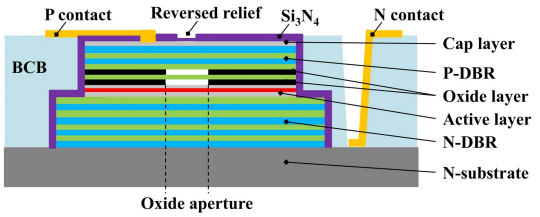


Fig. 1. Schematic cross section of 880 nm VCSEL.

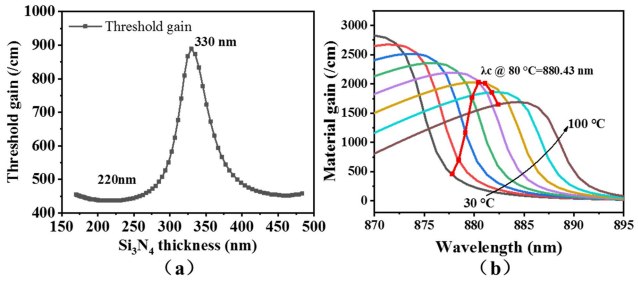


Fig. 2. (a) Variation in the threshold gain of the VCSEL with the thickness of $Si_3N_4$; (b) gain spectra of the quantum wells at different temperatures. The solid box indicates the cavity-mode gain with increasing temperature and the carrier density is $5 \times 10^{18}$ cm$^{-3}$.

gain of the VCSEL. According to the spatial distribution of different transverse modes in VCSEL, the threshold gain of the fundamental mode was reduced by etching part of the inversion layer in the position where the fundamental mode was more distributed. Fig. 2(a) shows the variation in the threshold gain with the thickness of the $Si_3N_4$ film. The thickness of the $Si_3N_4$ film was 220 nm at the center of the VCSEL where the fundamental modes were more distributed. The film thickness at the other positions were 330 nm to increase the threshold gain of higher order modes. The relief diameter was 3 $\mu$m. The detailed design method of reversed relief references [18]. The lasing wavelength of the VCSELs was determined by the resonance wavelength ($\lambda$c) in the cavity. Effective gain at $\lambda$c was called the cavity-mode gain. To achieve a high-temperature operation, a gain–cavity mode mismatch design was adopted [19]. The cavity mode gains at different temperatures are indicated by the solid red box in Fig. 2(b). The carrier density to calculate the gain spectrum was set to $5 \times 10^{18}$ cm$^{-3}$. VCSEL presented the maximum cavity-mode gain when the temperature range was 70 °C–80 °C and corresponded to the gain–cavity detuning of ∼10.6 nm at room temperature. The value of $\lambda$c was 880.43 nm at 80 °C.

## III. Static Characteristics at Room and High Temperature

The VCSEL for static characteristic testing was packaged in the form of TO56 and installed on a commercial laser diode mount to control the temperature and current. The current and temperature control accuracies were 0.001 mA and 0.01 °C, respectively. Fig. 3(a) depicts the power–injection current–voltage (P-I-V) characteristics of the 880-nm VCSEL at different temperatures under continuous wave (CW). The voltage of the VCSEL decreased slightly with the increase in temperature, and the device resistance from the I-V curve

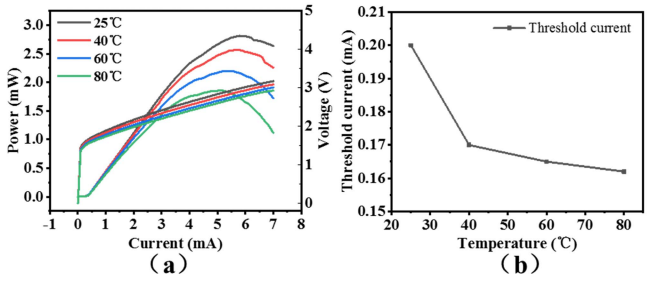


Fig. 3. (a) Static P- I-V characteristics of VCSELs at different temperatures; (b) variation in the threshold current with temperature.

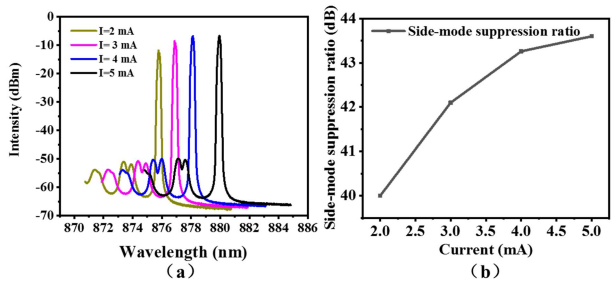


Fig. 4. (a) Measured spectra at 2 to 5 mA; (b) variation in the side-mode suppression ratio with current.

fitting was ∼240 Ω. The maximum output power dropped from 2.8 mW to 1.86 mW as the temperature increased from 25 °C to 80 °C. Fig. 3(b) shows the change in the threshold current with temperature. Due to the gain–cavity mode mismatch design, the threshold current of the device decreased as the temperature increased, reaching the lowest value of 0.162 mA at 80 °C. The spectral characteristic of the VCSEL at 25 °C under CW is shown in Fig. 4. At 25 °C, the side-mode suppression ratio (SMSR) at all tested currents were larger than 40 dB.

## IV. Small-Signal Analysis

Small-signal modulation response and reflection scattering were measured at different currents and operating temperatures. We used a 4-$\mu$m aperture VCSEL as an example for the measured small-signal modulation response curves at room temperature. The 3-dB frequencies reached maximum value at 5 mA and then started to decrease with further increase in the current. Same measurements and evaluation were performed at different temperatures. Fig. 5(a) illustrates the small-signal response of a VCSEL with a 4-$\mu$m oxide-aperture at driving currents of 3, 4, and 5 mA in the data transmission experiments at 25 °C. The −3-dB bandwidth $f_{-3\mathrm{dB}}$ is an important parameter for modulation, because it is directly related to the maximum achievable bitrate. Our VCSEL achieved 20.09, 21.35, and 22.53 GHz with bias currents of 3, 4, and 5 mA, respectively, at room temperature. Fig. 5(b) shows the small-signal modulation response at high temperature of 75 °C; that is, the bandwidths were 18.38, 21.96, and 21.47 GHz with bias currents of 3, 4, and 5mA, respectively. A decrease of only 1.06 GHz was observed at the highest modulation bandwidth, which showed high-temperature stability due to our special design of epitaxy. The VCSEL at room temperature had a higher speed than at higher temperatures, because the thermal effects introduced by

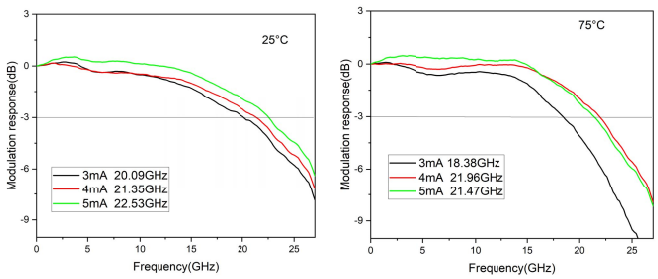


Fig. 5. Measured small-signal responses for different bias conditions at (a) 25 °C and (b) 75 °C.

Joule heating already led to a limitation. Our VCSELs showed very temperature-stable bandwidths with a small change of only 1.06 GHz over the temperature range from 25 °C to 75 °C (Fig. 5). The results showed a large flat range for the modulation response, which is very important for long-distance data transmission. The flat curves were obtained by optimizing the photon lifetime. To maximize the −3 dB bandwidth of VCSEL, lower damping of the relaxation oscillation is required, which need a higher cavity loss with a shorter photon lifetime. Although low damping is required to reach higher bandwidths in VCSELs, a certain amount of damping is needed to reduce ringing and timing jitter for high-speed data transmission. Thus, we needed to optimize the photon lifetime for high bandwidth and flat response with reasonable damping, instead of only large bandwidth, to reach data transmission over ∼500 m.

## V. Large-Signal Experiments

Data transmission of 880-nm SM-VCSELs was tested for the commercial scenario of 400G DR8. This scenario requires that the SM-VCSEL can support the transmission rate of 50 Gbit/s over a distance of 500 m. To verify whether our VCSEL can meet the requirement, we performed three-step data transmission experiments; That is, we transmitted data over 500 m at 25 Gbit/s with OM4 fiber, over 340 m at 50 Gbit/s with OM4 fiber, and 500 m at 50 Gbit/s with G652D fiber.

A 25G NRZ module was encapsulated using the SM-VCSEL by replacing the multi-mode 850-nm VCSEL chip of the transmitter in the current commercial module with our 880 nm SM-VCSEL chip. As shown in Fig. 6(a), the module had a transmitter and a receiver corresponding to the output port of the 880-nm SM-VCSEL and the receiving port of the PD. We fused the output port of the 880-nm SM-VCSEL to a 500-m OM4 fiber and then tested the eye diagram and bit error rate. Fig. 6(b) illustrates the eye diagram of the BTB transmission at 25 Gbit/s, and Fig. 6(c) shows that at 25 Gbit/s after 500 m transmission. The received power was −2.71dBm, and the error ration was 5.3e−7. The back-to-back (B2B) eye diagrams at 25 Gbps did not show any distortion related to the nonlinearities of the VCSEL itself. The extinction ratio (ER) of the B2B NRZ eyes is 3.7 dB.

A 50G PAM4 module was also packaged with our SM-VCSEL. A commercial DSP chip was used to package a 400G DR module, as shown in Fig. 7(a). The module had four 880-nm SM-VCSEL output ports and four PD receiving ports.

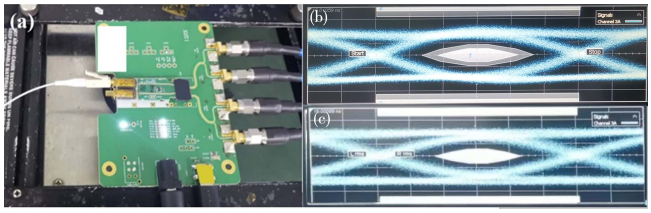


Fig. 6. (a) The module included a transmitter and a receiver corresponding to the output port of the 880-nm SM-VCSEL and the receiving port of the PD; eye diagrams of the (b) BTB transmission at 25 Gbit/s and (c) at 25 Gbit/s after transmission over 500 m. The received power was −2.71dBm, and the error ration was 5.3e−7.

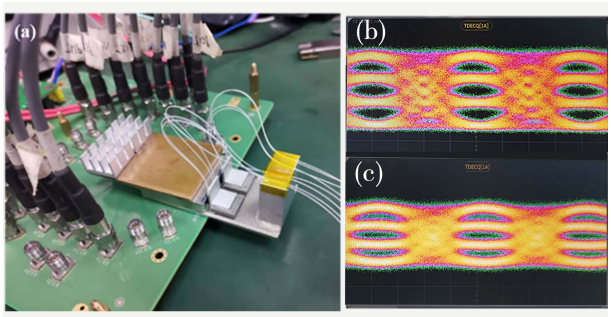


Fig. 7. (a) Packaged 50G PAM4 module with our SM-880nm VCSEL; (b) Eye diagrams of the BTB data transmission at 50 Gbit/s (c) eye diagram after 500m G652D fiber data transmission, with the error ratio of 2.8e-6.

The modulation amplitude of the signal driving the VCSEL for the PAM 4 transmisson was adjusted to stay in the linear region of the output power to drive the current relationship (the P-I relationship). Nopredistortion or equalization was done to the signal. The eye diagrams of BTB data transmission at 50 Gbit/s is shown in Fig.7(b). After the output port of the 880-nm SM-VCSEL was fused to a 500-m long G652D fiber, the eye diageam test was repeated. A fiber lens was fabricated at the end of a special 850-band single-mode fiber, and the coupling loss between SM-VCSEL and the fiber was about 0.7dB. In addition, the fusion loss between special 850 single-mode fiber and G652D is less than 0.3dB, so the coupling loss between SM-VCSEL and G652D is less than 1.0 dB. Fig. 7(c) shows the eye diagram after data transmission over 500 m, with the error ratio of 2.8e−6. Some other impairments could be observed from the eye diagrams. The highest power modulation level was broadened, possibly due to the RIN or modal noise, because more modes were excited in the VCSEL as the output power increased. Level splitting was observed at the top level.

## VI. Conclusion

Integrating the SR mode filters on high-speed, oxide-confined, 880-nm VCSELs enabled single transverse mode operation with narrow spectral width and relatively high output power. Error-free data transmissions up to 500 m at 50 Gbit/s were demonstrated with the record bitrate–distance product of 25 (Gbit/s)•km. A 50 Gbit/s single-channel transmission over 500 nm was achieved using directly modulated 880-nm SM-VCSELs. This result indicated that 400G DR8 module could be realized by combining SM-VCSELs and the 4-channel packaging method. This scheme presented obvious cost and power consumption advantages over current DML solution, which is the commonly used 400G DR8 module.

## References

[1] K. Szczerba, P. Westbergh, E. Agrell, M. Karlsson, P. A. Andrekson, and A. Larsson, "Comparison of intersymbol interference power penalties for OOK and 4-PAM in short-range optical links," *J. Lightw. Technol.*, vol. 31, no. 22, pp. 3525–3534, Nov. 22, 2013.

[2] K. Szczerba *et al.*, "30 Gbps 4-PAM transmission over 200m of MMF using an 850 nm VCSEL," *Opt. Exp.*, vol. 19, no. 26, p. B203, Dec. 2011.

[3] K. Szczerba, P. Westbergh, M. Karlsson, P. A. Andrekson, and A. Larsson, "60 Gbits error-free 4-PAM operation with 850 nm VCSEL," *Electron. Lett.*, vol. 49, no. 15, pp. 953–955, Jul. 2013.

[4] K. Szczerba *et al.*, "70 Gbit/s 4-PAM and 56 Gbit/s 8-PAM using an 850 nm VCSEL," *J. Lightw. Technol.*, vol. 33, no. 7, pp. 1395–1401, Apr. 1, 2015.

[5] K. Szczerba, T. Lengyel, M. Karlsson, P. A. Andrekson, and A. Larsson, "94-Gb/s 4-PAM using an 850-nm VCSEL, pre-emphasis, and receiver equalization," *IEEE Photon. Technol. Lett.*, vol. 28, no. 22, pp. 2519–2521, Nov. 15, 2016.

[6] J. Lavrencik *et al.*, "100 Gbit/s PAM-4 transmission over 100m OM4 and wideband fiber using 850 nm VCSELs," in *Proc. 42nd Eur. Conf. Opt. Commun.*, 2016, pp. 1–3.

[7] C. Y. Huang *et al.*, "Multimode VCSEL enables 42 GBaud PAM-4 and 35 GBaud 16-QAM OFDM for 100-m OM5 MMF data link," *IEEE Access*, vol. 8, pp. 36963–36973, 2020.

[8] M. J. Li *et al.*, "SM-VCSEL transmission for short reach communications," *J. Lightw. Technol.*, vol. 39, pp. 868–880, Feb. 15, 2021.

[9] H.-Y. Kao *et al.*, "Modal linewidth dependent transmission performance of 850-nm VCSELs with encoding PAM-4 over 100-m MMF," *IEEE J. Quantum Electron.*, vol. 53, no. 5, pp. 1–8, Oct. 2017.

[10] J. Qiu, X. Yu, and M. Feng, "85 °C operation of single-mode 850 nm VCSELs for high speed error-free transmission up to 1 km in OM4 fiber," in *Proc. Opt. Fiber Commun. Conf. (OFC)*. San Diego, CA, USA: Optical Society of America, 2019, pp. 3–7.

[11] C.-Y. Peng, J. Qiu, T.-Y. Huang, C.-H. Wu, M. Feng, and C.-H. Wu, "850-nm single-mode vertical-cavity surface-emitting lasers for 40 Gb/s error-free transmission up to 500 m in OM4 fiber," *IEEE Electron Device Lett.*, vol. 41, no. 1, pp. 84–86, Jan. 2020.

[12] H. J. Unold, S. W. Z. Mahmoud, R. Jager, M. Grabherr, R. Michalzik, and K. J. Ebeling, "Large-area single-mode VCSELs and the self-aligned surface relief," *IEEE J. Sel. Topics Quantum Electron.*, vol. 7, no. 2, pp. 386–392, 2001.

[13] D.-S. Song, S.-H. Kim, H.-G. Park, C.-K. Kim, and Y.-H. Lee, "Single-fundamental-mode photonic-crystal vertical-cavity surface-emitting lasers," *Appl. Phys. Lett.*, vol. 80, no. 21, pp. 3901–3903, May 2002.

[14] Y. J. Yang, T. G. Dziura, T. Bardin, S. C. Wang, and R. Fernandez, "Continuous-wave single-transverse-mode vertical-cavity surface-emitting lasers fabricated by helium Implantation and zinc diffusion," *Electron. Lett.*, vol. 28, pp. 274–276, May 1992.

[15] *40G SWDM4 MSA Technical Specifications*. [Online]. Available: http://www.swdm.org/wp-content/uploads/2017/11/40G-SWDM4-MSA-Technical-Spec-1-0-1.pdf

[16] R. Michalzik, *Fundamentals, Technology and Applications of Vertical-Cavity Surface-Emitting Lasers* (Optical Sciences), vol. 166. Ulm, Germany: Springer, 2013.

[17] Y. Zhou *et al.*, "Large-aperture single-mode 795 nm VCSEL for chip-scale nuclear magnetic resonance gyroscope with an output power of 4.1 mW at 80° C," *Opt. Exp.*, vol. 30, no. 6, pp. 8991–8999, 2022.

[18] L. Xiang *et al.*, "VCSEL mode and polarization control by an elliptic dielectric mode filter," *Appl. Opt.*, vol. 57, no. 28, pp. 8467–8471, 2018.

[19] J. W. Zhang, X. Zhang, H. B. Zhu, Y. Q. Ning, L. Qin, and L. J. Wang, "High-temperature operating 894.6 nm-VCSELs with extremely low threshold for Cs-based chip scale atomic clocks," *Opt. Exp.*, vol. 23, pp. 14763–14773, Jun. 2015.